# Most probable paths for active Ornstein-Uhlenbeck particles

Sandipan Dutta*

*Department of Physics, Birla Institute of Technology and Science, Pilani, Rajasthan, 333031, India*

(Received 8 August 2022; revised 7 April 2023; accepted 5 May 2023; published 25 May 2023)

Fluctuations play an important role in the dynamics of stochastic systems. In particular, for small systems, the most probable thermodynamic quantities differ from their averages because of the fluctuations. Using the Onsager Machlup variational formalism we analyze the most probable paths for nonequilibrium systems, in particular, active Ornstein-Uhlenbeck particles, and investigate how the entropy production along these paths differs from the average entropy production. We investigate how much information about their nonequilibrium nature can be obtained from their extremum paths and how these paths depend on the persistence time and their swim velocities. We also look at how the entropy production along the most probable paths varies with the active noise and how it differs from the average entropy production. This study would be useful to design artificial active systems with certain target trajectories.

DOI: 10.1103/PhysRevE.107.054130

## I. INTRODUCTION

Active matter is a new class of nonequilibrium systems in condensed matter which constantly dissipates energy to produce motion [1–4]. The flocking of birds and fish and the swimming of organisms are examples of active matter systems [5]. Many artificial motile systems like Janus colloids [6–8], colloidal rollers [9], and water droplets [10,11] were developed that mimic these biological systems. Several models were used to study active systems like the active Brownian particle [12–14], run and tumble [15–17], and active Ornstein-Uhlenbeck particle (AOUP) model [18–21]. AOUP is one of the simplest models where the velocities of the active particles are exponentially correlated in time and are modeled using the Langevin equations with colored noise. All these models were able to explain the collective behavior of active systems like motility-induced phase separation [16,22–24] through a combination of motility and steric repulsion. While most studies on active matter looked at their collective behavior, here we focus on the thermodynamics along the trajectories of a single active particle.

In many of these systems, the correlated noise like the Ornstein-Uhlenbeck (OU) noise induces stochastic transitions between possible states, as in the case of chemical reactions [25,26]. Many of these transitions in the two state systems are induced by noise. These stochastic transitions are rare with a very low probability like a microswimmer passing through a slit [27] and escaping from a capture near a wall [28]. These rare events help microorganisms in their survival. Finding the most probable trajectory between two given points is one of the key problems in rare events [29–33]. The path probability along with the Onsager-Machlup (OM) integral are useful tools to calculate the most probable path (MPP) for arbitrary initial and final states [34–38]. The MPP of transitions have been studied in a double-well potential [32], experiments [39], protein folding [31,40], and chemical reactions [33]. Interest in the MPPs in active systems is very recent [41]. Yasuda and Ishimoto recently showed that the extremum path of a single active Brownian particle was analogous to the pendulum equation. They obtained multiple extremum paths of which they found the U-shaped path to be most probable.

In this work, we find the MPP for a system of AOUP particles from the extremum of the OM integral. We focus on the case of noninteracting AOUP particles for which the MPPs are analytically solvable for all types of boundary conditions unlike ABP particles [41] and obtain their phase diagram. Our primary objective is to investigate how much information about the nonequilibrium nature of the AOUP is contained in their extremum trajectories. We look at how the trajectories differ at different regions of the phase space. We find that the AOUP has an unstable fixed point and study its dynamics around that fixed point. We then consider the entropy production for the MPP. The entropy production quantifies the time irreversibility of the nonequilibrium systems [42] and is obtained from the ratio of the probabilities of the forward and backward trajectories [43]. It was suggested [42] that the OU noise can have different parities under time reversal in the context of active particles in a thermal bath or second, a passive particle in an active bath. The OU noise is odd under time reversal [42] for an active AOUP particle in an equilibrium thermal bath [44–47] and even for a passive particle in an active AOUP bath [19,48–56]. Accordingly, the entropy productions are different in these cases. Here we consider both the parities and compare the differences in behavior. We also compare the entropy production along the MPP with the average entropy production.

In the next section, we write the stochastic dynamics of AOUP particles. The MPP is derived from the OM integral for the AOUP system in Sec. III and the phase space of solutions is obtained in Sec. IV for the case of a single AOUP particle.

*sandipan.dutta@pilani.bits-pilani.ac.in

 

We calculate the entropy production along the most probable and extremum trajectories in Sec. V and compare it with the average entropy production. Finally we conclude in Sec. VI.

## II. ACTIVE ORNSTEIN-UHLENBECK PARTICLE MODEL

Consider an active particle suspended in a thermal bath of temperature $T$. The particle experiences a conservative force $-\nabla U(\mathbf{x})$ in addition to active forces $\boldsymbol{\eta}$ from their intrinsic self-propulsion. $U$ is the potential energy of a conservative force due to the interactions with other particles as well as some external potential and $\mathbf{x}$ is the position of the particle. This description applies to both cases of a passive particle in an active bath or an active particle in a passive bath.

We consider the overdamped Langevin equation [57,58] for the particle

$$\dot{\mathbf{x}}(t) = \mathbf{f}[\mathbf{x}(t), t] + \sqrt{2D_a}\boldsymbol{\eta}(t) + \sqrt{2D}\boldsymbol{\xi}(t), \tag{1}$$

where $\mathbf{f}(\mathbf{x}, t) = -\frac{1}{\gamma}\nabla U(\mathbf{x}, t)$ and $\gamma$ is the hydrodynamic friction. $\boldsymbol{\xi}(t)$ are the thermal fluctuations which are Gaussian with zero mean and delta function correlations $\langle \xi_\alpha(t)\xi_\beta(t')\rangle = \delta_{\alpha\beta}\delta(t-t')$, where $\alpha$ and $\beta$ are the Cartesian indices. $D = k_BT/\gamma$ is the diffusion constant in the thermal bath and $D_a$ is the diffusion constant due to activity. The active fluctuations $\boldsymbol{\eta}$ are OU processes with zero mean and exponential correlations

$$\langle \eta_\alpha(t)\eta_\alpha(t')\rangle = \frac{\delta_{\alpha\beta}}{2\tau}\exp(-|t-t'|/\tau). \tag{2}$$

$\tau$ is the persistence time that quantifies the persistence of the active fluctuations. The active diffusion constant can be written as $D_a = v_0^2\tau$ where $v_0$ is the swim velocity of the active particle [59]. These equations are easily generalized to $N$ identical particles with positions $\{\mathbf{x}_i\}$ with the same parameters $D$ and $D_a$. The active noise for two particles satisfies $\langle \eta_{i\alpha}\eta_{j\beta}\rangle = \frac{\delta_{\alpha\beta}\delta_{ij}}{2\tau}\exp(-|t-t'|/\tau)$, where $i$, $j$ are particle indices.

## III. MOST PROBABLE TRAJECTORY

Let $\mathbf{y} = (\mathbf{x}, \boldsymbol{\eta})$ denote the combined variable of the particle position and the active noise. The probability of observing certain trajectory of the Markovian process $\mathbf{y}(s)|_0^t$ starting at $\mathbf{y}_0$ at $s = 0$ and ending at $\mathbf{y}_f$ at $s = t$ is given by the Onsager-Machlup path integral [34,35] by

$$p[\mathbf{y}(t)|\mathbf{y}_0] \propto \exp\Bigg[-\int_0^t \frac{ds}{4}\sum_{i,j}\sum_{\alpha,\beta}\{f_{i\alpha}[\mathbf{y}(s)] - \dot{y}_{i\alpha}\} \times D^{-1}_{i\alpha,j\beta}\{f_{j\beta}[\mathbf{y}(s)] - \dot{y}_{j\beta}\}\Bigg]. \tag{3}$$

$y_{i\alpha}$ denotes the $\alpha$ component of variable $\mathbf{y}$ for the particle $i$. $D_{i\alpha,j\beta}$ is the diffusion tensor that is diagonal in our case. This equation is derived in Appendix A following Refs. [41,60]. For the Langevin equation (1) summing over $\alpha$, $\beta$ and putting the explicit form of $\mathbf{y}$ in terms of $\mathbf{x}$ and $\boldsymbol{\eta}$ and the diffusion matrix (Appendix A), we get [42,61]

$$p(\mathbf{x}, \boldsymbol{\eta}|\mathbf{x}_0, \boldsymbol{\eta}_0) \propto \exp\left(-\int_0^t ds\sum_{i=1}^N\left[\frac{[\dot{\mathbf{x}}_i(s) - \mathbf{f}_i(s) - \sqrt{2D_a}\boldsymbol{\eta}_i(s)]^2}{4D} + \frac{[\tau\dot{\boldsymbol{\eta}}_i(s) + \boldsymbol{\eta}_i(s)]^2}{2} + \frac{1}{2}\nabla\cdot\mathbf{f}_i(s)\right]\right). \tag{4}$$

The last term in the exponent occurs from the indeterminacy of the time discretization [41].

The quantity inside the exponent of the OM integral is similar to a Lagrangian and we denote it by

$$L(\mathbf{x}, \dot{\mathbf{x}}, \boldsymbol{\eta}, \dot{\boldsymbol{\eta}}) = \sum_{i=1}^N \frac{[\dot{\mathbf{x}}_i(s) - \mathbf{f}_i(s) - \sqrt{2D_a}\boldsymbol{\eta}_i(s)]^2}{4D} + \frac{[\tau\dot{\boldsymbol{\eta}}_i(s) + \boldsymbol{\eta}_i(s)]^2}{2} + \frac{1}{2}\nabla\cdot\mathbf{f}_i(s). \tag{5}$$

The extremum paths are obtained by the variation of the OM integral and setting the first variation to zero

$$\frac{d}{dt}\frac{\delta}{\delta\dot{y}_{i\alpha}(t)}L(\mathbf{x}, \dot{\mathbf{x}}) - \frac{\delta}{\delta y_{i\alpha}(t)}L(\mathbf{x}, \dot{\mathbf{x}}) = 0, \tag{6}$$

which from Eq. (5) gives

$$\frac{1}{2D}\left(\ddot{x}_{i\alpha} - \frac{d}{dt}f_{i\alpha} - \sqrt{2D_a}\dot{\eta}_{i\alpha}\right) = -\frac{1}{2D}\partial_{i\alpha}f_{j\beta}(\dot{x}_{j\beta} - f_{j\beta} - \sqrt{2D_a}\eta_{j\beta}) + \frac{1}{2}\partial_{i\alpha}\partial_{j\beta}f_{j\beta},$$

$$(\tau^2\ddot{\eta}_{i\alpha} + \tau\dot{\eta}_{i\alpha}) = (\tau\dot{\eta}_{i\alpha} + \eta_{i\alpha}) - \frac{\sqrt{2D_a}}{2D}(\dot{x}_{i\alpha} - f_{i\alpha} - \sqrt{2D_a}\eta_{i\alpha}). \tag{7}$$

These coupled equations are solved to obtain the extremum paths. The second variation of the OM integral should be positive for the probability to be maximum along the extremum path.

## IV. FREE ACTIVE AOUP PARTICLES

The MPP in Eq. (7) can be solved analytically in the case of free AOUP particles for which $\mathbf{f} = 0$. The equations of motion of the particles decouple from one another because of the absence of the interactions. The motion along the $x$, $y$, and $z$ coordinates also decouples due to the nature of OU noise. Thus for the free AOUP system we will focus on the dynamics of a single particle in one dimension.

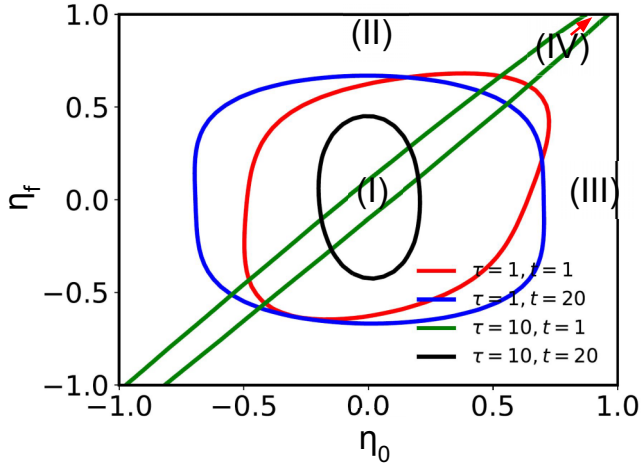


FIG. 1. The constant $L = 0.5$ curves for different initial and final active noise parameters $\eta_0$ and $\eta_f$. The paths that satisfies Eq. (8) and $L \approx 0$ would give the MPPs. $t$ is the travel time for the particle to reach $x(t) = 1$ from the origin $x(0) = 0$ and persistence times $\tau$. The other parameters are fixed at $D = 1$ and $D_a = 5$. We plot the trajectories at the points (I) $\eta_0 = 0$, $\eta_f = 0$, (II) $\eta_0 = 0$, $\eta_f = 1$, (III) $\eta_0 = 1$, $\eta_f = 0$, and (IV) $\eta_0 = 5$, $\eta_f = 5$ in Fig. 2.

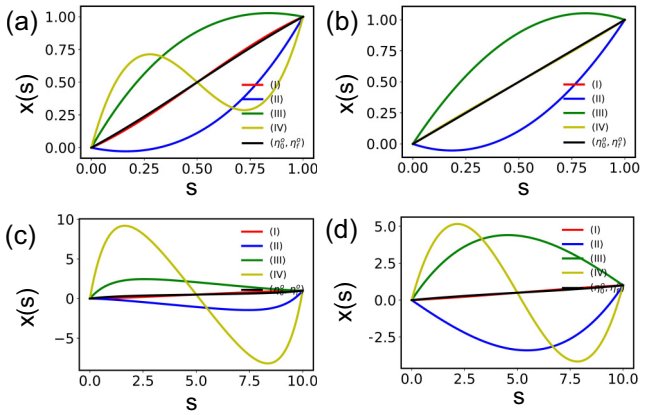


FIG. 2. The extremum paths of the AOUP between $x(0) = 0$ and $x(t) = 1$ at the points (I), (II), (III), and (IV) in Fig. 1 for short time $t = 1$ : (a) $\tau = 1$, (b) $\tau = 10$, and long time $t = 10$ : (c) $\tau = 1$, and (d) $\tau = 10$. Also shown are the MPPs for parameters ($\eta_0 = \eta_0^o$, $\eta_f = \eta_f^o$) of which $L$ function is minimum.

### Most probable path in one dimension

The extremum path for a single AOUP particle in one dimension is given by

$$\ddot{x} - \sqrt{2D_a}\dot{\eta} = 0,$$
$$\tau^2\ddot{\eta} = \eta - \frac{\sqrt{2D_a}}{2D}(\dot{x} - \sqrt{2D_a}\eta). \tag{8}$$

Since the entire derivation is based on the use of translational probability in Eq. (3), we only solve for the trajectories with a fixed start $x(0) = x_0$ and end point $x(t) = x_f$ for a travel time $t$. The active noise also has fixed boundaries $\eta(0) = \eta_0$ and $\eta(t) = \eta_f$. The solution gives the extremum trajectory of the particle, which is nothing but the local minimum of the function $L$ in Eq. (8). For the rest of the discussions we explore the behavior of the extremum paths of the particle that always start at the origin $x_0 = 0$ and ends at $x_f = 1$. The exact analytical solutions are obtained using MATHEMATICA software [62] for $x(t)$ and $\eta(t)$ and are given in Appendix B. These solutions are the local minimum of the $L$ function. To obtain the global minimum of $L$ for the MPPs, we search the phase space of the parameters $\eta_0$ and $\eta_f$ keeping the other parameters $D_a$, $D$, and $\tau$ fixed. Since $L \geqslant 0$ for a free AOUP particle, the global minimum is expected to be $L \approx 0$. From now on we fix the diffusion constants $D = 1$ and $D_a = 5$. The space of solutions of the MPP for which $L \approx 0$ lies inside of the closed curves of Fig. 1. As we increase the persistence time $\tau$, the solution space of the MPP shifts closer to the origin and the area inside the curve decreases. This implies that the MPP at large $\tau$ is obtained for very small active noise parameters $\eta_0 \approx 0$ and $\eta_f \approx 0$.

In Fig. 2 we look at the trajectories at different regions of the $(\eta_0, \eta_f)$ space, in particular at the four points (I), (II), (III), and (IV) in Fig. 1. We numerically obtain the optimal noise parameters $(\eta_0^{(o)}, \eta_f^{(o))})$ that give the smallest values of the $L$ function for short trajectory time $t = 1$ in Figs. 2(a) and 2(b) and for long time $t = 20$ in Figs. 2(c) and 2(d). For points (I) and (IV) along the $\eta_0 = \eta_f$ line in Fig. 1, the trajectories oscillate about the straight line joining the end points $x(0) = 0$ and $x(t) = 1$ and cross at $t/2$. For $\eta_0 > \eta_f$ (III) the trajectories are above the straight line while for $\eta_0 < \eta_f$ (II) they remain below. $\eta_0 = 0, \eta_f = 0$ is always a good approximation for the MPP. Larger $L$ values result in longer trajectories and deviation from the straight line or the MPP. For low $\tau$ the AOUP has larger swim velocity, thus reaching the end point faster than for large $\tau$. As seen from Fig. 1 at large $\tau$, the optimal noise becomes zero thus slowing the particle down. The most probable trajectory of a passive particle between two points $x_0$ and $x_f$ is obtained by taking the $D_a \to 0$ limit in Eq. (B1):

$$x(s) = \left(1 - \frac{s}{t}\right)x_0 + \frac{s}{t}x_f. \tag{9}$$

In the large $\tau$ limit Eq. (B1) reads

$$x(s) = \left(1 - \frac{s}{t}\right)x_0 + \frac{s}{t}x_f + \sqrt{2D_a}\frac{s}{2}\left(\frac{s}{t} - 1\right)(\eta_f^{(o)} - \eta_0^{(o)}). \tag{10}$$

Since $\eta_0^{(o)} \approx 0$ and $\eta_f^{(o)} \approx 0$ from Fig. 1, MPP Eq. (10) at large $\tau$ coincides with the MPP of the passive particle in Eq. (9). This is also observed in all the plots in Fig. 2, as $\tau$ increases it coincides with the straight line joining $x_0$ and $x_f$. This can be understood from the fact that, as the persistence time $\tau$ increases for a fixed $D_a$, the swim velocity $v_0 = \sqrt{D_a/\tau}$ decreases. Thus the AOUP behaves like a passive particle at large $\tau$. While for large $t$ [Fig. 2(d)] even a small perturbation of the noise from the optimal noise produces a large deviation from the MPP, for short time $t = 1$ [Fig. 2(b)] the particle does not get enough time to deviate appreciatively from the MPP.

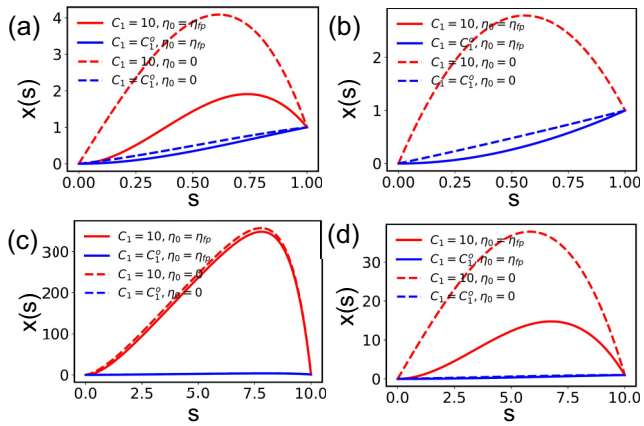


FIG. 3. The extremum path for $C_1 = 10$ and the MPP of the AOUP near the fixed point $\eta_{fp}$ of Eq. (11) for (a) $t = 1, \tau = 1$, (b) $t = 1, \tau = 10$, (c) $t = 10, \tau = 1$, and (d) $t = 1, \tau = 10$.

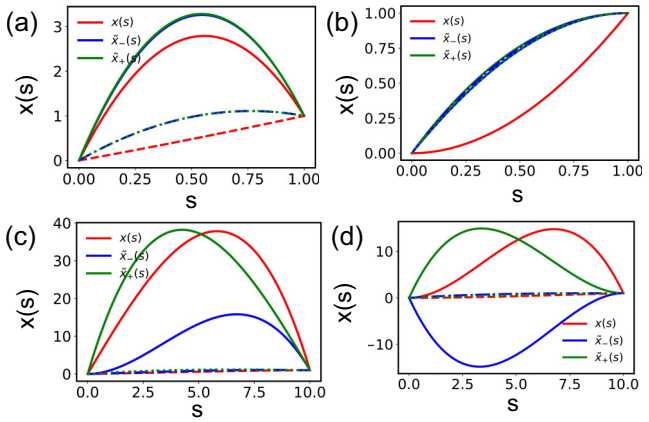


FIG. 4. The time reversed trajectories in Eq. (14) corresponding to the two parities for $\tau = 10$ and $C_1 = 10$. Trajectories in (a) and (c) do not pass through the fixed point with $\eta(0) = 0$ and in (b) and (d) pass through the fixed point. (a,b) $t = 1$ and (c,d) $t = 10$.

We analyze the fixed point dynamics of the AOUP. We rewrite Eq. (8) as

$$v_x - \sqrt{2D_a}\eta = C_1,$$
$$\tau^2 v_\eta \frac{dv_\eta}{d\eta} = \eta - \frac{\sqrt{2D_a}}{2D}C_1, \tag{11}$$

where $v_x = \dot{x}$, $v_\eta = \dot{\eta}$, and $C_1$ is a constant of integration. $C_1$ is the velocity of the particle in the absence of active noise. The drift of the AOUP particle is caused by the active noise and has an unstable fixed point at $\eta_{fp} = -C_1/\sqrt{2D_a}$. The dynamics of the active noise evolves independently of the particle position or velocity because of translational invariance. The second equation of Eq. (11) is integrated to obtain

$$v_\eta^2 = V_0^2 + \frac{1}{\tau^2}\left(\eta - \frac{\sqrt{2}D_a}{2D}C_1\right)^2. \tag{12}$$

$V_0$ is the velocity at $\eta = \frac{\sqrt{2}D_a}{2D}C_1$. In Fig. 3 we see that the extremum trajectories passing through the fixed point $\eta = \eta_{fp}$ are less spread out as the active noise and hence the velocity of the AOUP is smaller. The MPPs for all $t$ and $\tau$ are always close to the passive trajectory of the straight line 9. When $t \approx \tau$, the trajectories have similar behavior in Figs. 3(a) and 3(d) except the trajectories are more spread out in Fig. 3(d) where $t$ is large. For smaller $\tau$ and large $t$ in Fig. 3(c) the swim velocity is large and especially for large $C_1$ the trajectories spread out significantly.

## V. ENTROPY PRODUCTION FOR AOUP PARTICLES

The nonequilibrium nature of active systems is reflected in the time irreversibility of their trajectories. This is quantified by the entropy production which is the ratio of the probabilities of the forward and the backward paths [43]

$$\exp(\Sigma) = \frac{p(\mathbf{x}, \boldsymbol{\eta}|\mathbf{x}_0, \boldsymbol{\eta}_0)}{\tilde{p}(\tilde{\mathbf{x}}, \tilde{\boldsymbol{\eta}}|\tilde{\mathbf{x}}_0, \tilde{\boldsymbol{\eta}}_0)}. \tag{13}$$

To obtain the time-reversed trajectory for a time interval $t$, we are left with the choice of the noise $\boldsymbol{\eta}$ being even or odd under time reversal $\tilde{\boldsymbol{\eta}}_\pm(s) = \pm\boldsymbol{\eta}(t - s)$. The authors of Ref. [42] interpreted the active fluctuations as external forces to have even parity for passive particles in an active bath, while having odd parity for the case of self-propelled particles representing the velocity of the particle. This interpretation of parity was contested in Ref. [63]. The authors of Ref. [64] obtained the entropy production without explicit assumptions about the parity under time reversal. Here we consider both the parities for the active noise and analyze the time-reversed trajectories in both cases. The time-reversed trajectories according to the two parities, $x_-(x_+)$ for odd (even) parity, of the active noise are

$$-\dot{\tilde{x}}_-(s) + \sqrt{2D_a}\tilde{\eta}_-(s) = C_1,$$
$$\tau^2\ddot{\tilde{\eta}}_-(s) = -\tilde{\eta}_-(s) - \frac{\sqrt{2D_a}}{2D}C_1,$$

$$-\dot{\tilde{x}}_+(s) - \sqrt{2D_a}\tilde{\eta}_+(s) = C_1,$$
$$\tau^2\ddot{\tilde{\eta}}_+(s) = \tilde{\eta}_+(s) - \frac{\sqrt{2D_a}}{2D}C_1. \tag{14}$$

The plot of the time-reversed trajectories under odd and even parities are shown in Fig. 4. When $t < \tau$ both time-reversed trajectories are the same regardless of whether they are passing through the fixed point [Figs. 4(a) and 4(b)]. They are very different when $t \approx \tau$ as seen in Figs. 4(c) and 4(d). In the odd parity case, the entropy production from Eq. (13) reads [42]

$$\Sigma_- = \int_0^t ds\left[\frac{1}{D}\mathbf{f}(s)(\dot{\mathbf{x}}(s) - \sqrt{2D_a}\boldsymbol{\eta}(s)) - 2\tau\dot{\boldsymbol{\eta}}(s)\boldsymbol{\eta}(s)\right]. \tag{15}$$

In particular, for a free active particle in one dimension we get

$$\Sigma_-(t) = -\int_0^t ds 2\tau\dot{\eta}(s)\eta(s) = \tau\left(\eta_0^2 - \eta_f^2\right). \tag{16}$$

We recover the passive trajectory in Eq. (9) in the large $\tau$ limit of the MPP in Eq. (10) when $\eta_0 \approx 0$ and $\eta_f \approx 0$. Equation (16) too shows that the entropy production is zero along the MPP. Using $\langle\dot{\eta}(s)\eta(s)\rangle = -\frac{1}{2\tau^2}$ [42], we get $\langle\Sigma_-(t)\rangle = \frac{t}{\tau}$.

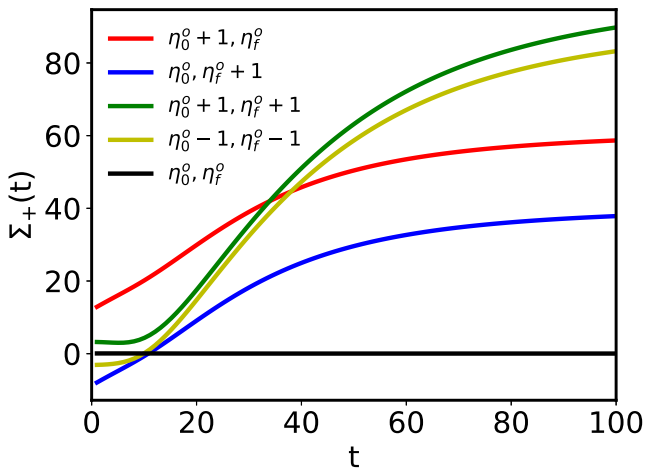


FIG. 5. The entropy production along the MPP (black) for $\tau = 100$ with optimal noises $(\eta_0^{(o)}, \eta_f^{(o)})$ as in Fig. 2 and the extremum paths with suboptimal noises.

In the case of even parity, the entropy production from Eq. (13) becomes

$$\Sigma_+ = \int_0^t ds\left[\frac{1}{D}\dot{\mathbf{x}}(s)(\mathbf{f}(s) + \sqrt{2D_a}\boldsymbol{\eta}(s)) - 2\tau\dot{\boldsymbol{\eta}}(s)\boldsymbol{\eta}(s)\right], \tag{17}$$

which for the free active particle in one dimension is

$$\Sigma_+ = \int_0^t ds\left[\frac{1}{D}\dot{x}(s)\sqrt{2D_a}\eta(s) - 2\tau\dot{\eta}(s)\eta(s)\right]. \tag{18}$$

Entropy production is a measure of how far the system is from equilibrium. In the long time limit $t \to \infty$, the entropy production from Eq. (18) along the extremum trajectories in Eq. (B1) saturates as seen in Fig. 5. Similar to the behavior of $\Sigma_-$ in Eq. (16) vanishes along the MPP, $\Sigma_+$ also vanishes along the MPP as seen in Fig. 5(a). This is because the optimal noise $(\eta_0^{(o)}, \eta_f^{(o)})$ is small at large $\tau$ (Fig. 1) in which case we recover the passive particle in a thermal bath limit as discussed in Sec. II. Thus for large $\tau$, the system behaves as an equilibrium system for which entropy production is zero. athe larger the deviation from the optimal noise, the larger is the entropy production thus driving the system away from equilibrium. The average entropy production $\langle\Sigma_+(t)\rangle = (1 + \frac{D_a}{D})\frac{t}{\tau}$ as derived in Appendix C increases linearly with time very different from the saturation behavior of $\Sigma_+$ which is a result of fixed end points.

## VI. CONCLUSION

We studied the MPP for AOUP active systems. OM formalism was used to obtain the transition probabilities of these systems. The extremum of the OM integral was then obtained using the variational principle similar to the Lagrange equation in classical mechanics to obtain the extremum path of the AOUP particles. Out of all the extremum paths, the MPPs are the ones that have the minimum OM integral value.

Free AOUP dynamics is analytically solvable. The extremum paths were solved for fixed start and end points of the trajectories, $x_0$ and $x_f$, and fixed start and end OU noise $\eta_0$ and $\eta_f$. We explored the phase space of the extremum paths by varying the persistence time $\tau$ and the noise $\eta_0$ and $\eta_f$ keeping the diffusion constants $D$ and $D_a$ constant. Unlike a passive particle which moves in a straight line from $x_0$ and $x_f$, the AOUP particle followed a curved path which approached the passive trajectory at large $\tau$. The AOUPs with higher swim velocities deviated more from the straight line trajectories. The AOUP had an unstable fixed point which depended only on the active noise and particles passing through the fixed point slows down resulting in less curved trajectories. The entropy production along the extremum trajectories saturated to a maximum value, unlike the average noise that increased linearly with time. The active noise can be odd or even under time reversal and accordingly the trajectories of the AOUP were different. We also looked at the differences in entropy production along both types of trajectories. This work would be useful to control the trajectories of artificial active colloidal systems.

## ACKNOWLEDGMENTS

The author acknowledges financial support by Science and Engineering Research Board (SERB), Government of India (File SRG/2022/000598) and (File MTR/2022/000281). The author also acknowledges financial support from the Birla Institute of Technology and Science, Pilani (File PLN/AD/2022-23/3). The author also thanks DST-FIST for the computational resources provided to the Department of Physics, BITS Pilani.

## APPENDIX A: DERIVATION OF THE TRANSITION PROBABILITY

The combined variable $\mathbf{y} = (\mathbf{x}, \boldsymbol{\eta})$ for $N$ particles follows the Langevin equation by combining Eq. (1) and $\tau\dot{\boldsymbol{\eta}}_i(t) = -\boldsymbol{\eta}_i(t) + \boldsymbol{\xi}_i(t)$,

$$\dot{y}_{i\alpha} = F_{i\alpha} + \xi_{i\alpha}, \tag{A1}$$

with $F_i = (\mathbf{v}_i + \sqrt{2D_a}\boldsymbol{\eta}_i, -\frac{1}{\tau}\boldsymbol{\eta}_i)$. The Gaussian white noise $\langle\xi_{i\alpha}\rangle = 0$ and $\langle\xi_{i\alpha}(t)\xi_{j\beta}(0)\rangle = 2D_{i\alpha,j\beta}\delta(t)$, where $D_{i\alpha,j\beta} = 0$ is the diffusion tensor. Following Refs. [41,60] we obtain for the path probability of a given trajectory $\mathbf{y}(s)$ starting at $\mathbf{y}_0$ and ending at $\mathbf{y}(t)$ as

$$p[\mathbf{y}(t)|\mathbf{y}_0] \propto \exp\left[-\int_0^t \frac{ds}{4}\{F_{i\alpha}[\mathbf{y}(s)] - \dot{y}_{i\alpha}\} \times D^{-1}_{i\alpha j\beta}\{F_{j\beta}[\mathbf{y}(s)] - \dot{y}_{j\beta}\}\right]. \tag{A2}$$

For free AOUP particle the diffusion tensor is

$$D_{i\alpha j\beta} = \delta_{ij}\begin{pmatrix} D & 0 \\ 0 & 1 \end{pmatrix}, \tag{A3}$$

which gives Eq. (3) in the text.

## APPENDIX B: EXACT SOLUTION OF EQ. (8)

The solution for the extremum path and the corresponding noise of Eq. (8) that satisfies the boundary conditions read

$$\begin{aligned} x(s) =& \operatorname{csch}(t/(2\tau))^2[D_a\tau\{(-x_0+x_f)\cosh(s/\tau)+(x_0-x_f)\cosh[(s-t)/\tau]+(x_0+x_f)\\ &\times[-1+\cosh(t/\tau)]\}+D\sqrt{2D_a}\tau\{-\eta_f s+\eta_f t-s\eta_0-\eta_f t\cosh(s/\tau)+t\eta_0\cosh[(s-t)/\tau]\\ &+(\eta_f s+s\eta_0-t\eta_0)\cosh(t/\tau)\}+D[-tx_0+s(x_0-x_f)]\sinh(t/\tau)+D_a[-tx_0+s(x_0-x_f)]\\ &\times\sinh(t/\tau)+\sqrt{2}D_a^{3/2}\tau\{-\eta_f s+\eta_f t-s\eta_0-\eta_f t\cosh(s/\tau)+t\eta_0\cosh[(s-t)/\tau]+(\eta_f-\eta_0)\tau\\ &\times\sinh(s/\tau)+\cosh(t/\tau)[\eta_f s+s\eta_0-t\eta_0+(-\eta_f+\eta_0)\tau\sinh(s/\tau)]+2(\eta_f-\eta_0)\tau\sinh[s/(2\tau)]^2\\ &\times\sinh(t/\tau)\}]/\{4D_a\tau-2(D+D_a)t\coth[t/(2\tau)]\}, \end{aligned} \tag{B1}$$

while for the noise we get

$$\begin{aligned} \eta(s) =& e^{t/\tau}[2D_a(\eta_f+\eta_0)\tau+2D_a(\eta_f-\eta_0)\tau\cosh[(s-t)/\tau]-2D_a(\eta_f+\eta_0)\tau\cosh(t/\tau)\\ &+2(D+D_a)t[\eta_f-\eta_0\cosh(t/\tau)]\sinh(s/\tau)-\sqrt{2D_a}(x_0-x_f)\{-\sinh(s/\tau)+\sinh[(s-t)/\tau]\\ &+\sinh(t/\tau)\}+2\cosh(s/\tau)[D_a(-\eta_f+\eta_0)\tau+(D+D_a)t\eta_0\sinh(t/\tau)]]/[-(D+D_a)t-2D_a\tau\\ &+4D_a e^{t/\tau}\tau+e^{(2t)/\tau}[(D+D_a)t-2D_a\tau]]. \end{aligned} \tag{B2}$$

## APPENDIX C: AVERAGE ENTROPY PRODUCTION ALONG A TRAJECTORY

Applying the expression of the Langevin equation in Eq. (1) in one dimension for a single particle to Eq. (C1) we get

$$\begin{aligned} \langle\Sigma\rangle &= \int_0^t ds\frac{1}{D}\langle(\dot{x}(s)\sqrt{2D_a}\eta(s)-2\tau\dot{\eta}(s)\eta(s))\rangle\\ &= \int_0^t ds\frac{1}{\tau}\left(\frac{D_a}{D}+1\right)\\ &= \frac{t}{\tau}\left(\frac{D_a}{D}+1\right). \end{aligned} \tag{C1}$$

Here we use $\xi$ and $\eta$ in Eq. (1) are uncorrelated, and $\langle\eta(s)\eta(s'\rangle = \frac{1}{2\tau}\exp(-|s-s'|/\tau)$.


[1] M. C. Marchetti, J.-F. Joanny, S. Ramaswamy, T. B. Liverpool, J. Prost, M. Rao, and R. A. Simha, Hydrodynamics of soft active matter, Rev. Mod. Phys. **85**, 1143 (2013).

[2] C. Bechinger, R. Di Leonardo, H. Löwen, C. Reichhardt, G. Volpe, and G. Volpe, Active particles in complex and crowded environments, Rev. Mod. Phys. **88**, 045006 (2016).

[3] J. Elgeti, R. G. Winkler, and G. Gompper, Physics of microswimmers—single particle motion and collective behavior: A review, Rep. Prog. Phys. **78**, 056601 (2015).

[4] T. Vicsek and A. Zafeiris, Collective motion, Phys. Rep. **517**, 71 (2012).

[5] S. Ramaswamy, The mechanics and statistics of active matter, Annu. Rev. Condens. Matter Phys. **1**, 323 (2010)

[6] J. R. Howse, R. A. L. Jones, A. J. Ryan, T. Gough, R. Vafabakhsh, and R. Golestanian, Self-Motile Colloidal Particles: From Directed Propulsion to Random Walk, Phys. Rev. Lett. **99**, 048102 (2007).

[7] H.-R. Jiang, N. Yoshinaga, and M. Sano, Active Motion of a Janus Particle by Self-Thermophoresis in a Defocused Laser Beam, Phys. Rev. Lett. **105**, 268302 (2010).

[8] G. Volpe, I. Buttinoni, D. Vogt, H.-J. Kümmerer, and C. Bechinger, Microswimmers in patterned environments, Soft Matter **7**, 8810 (2011).

[9] A. Bricard, J.-B. Caussin, D. Das, C. Savoie, V. Chikkadi, K. Shitara, O. Chepizhko, F. Peruani, D. Saintillan, and D. Bartolo, Emergent vortices in populations of colloidal rollers, Nat. Commun. **6**, 7470 (2015).

[10] Z. Izri, M. N. van der Linden, S. Michelin, and O. Dauchot, Self-Propulsion of Pure Water Droplets by Spontaneous Marangoni-Stress-Driven Motion, Phys. Rev. Lett. **113**, 248302 (2014).

[11] S. Thutupalli, R. Seemann, and S. Herminghaus, Swarming behavior of simple model squirmers, New J. Phys. **13**, 073021 (2011).

[12] P. Romanczuk, M. Bär, W. Ebeling, B. Lindner, and L. Schimansky-Geier, Active Brownian particles, Eur. Phys. J.: Spec. Top. **202**, 1 (2012).

[13] B. ten Hagen, S. van Teeffelen, and H. Löwen, Brownian motion of a self-propelled particle, J. Phys.: Condens. Matter **23**, 194119 (2011).

[14] F. J. Sevilla and M. Sandoval, Smoluchowski diffusion equation for active brownian swimmers, Phys. Rev. E **91**, 052150 (2015).

[15] R. W. Nash, R. Adhikari, J. Tailleur, and M. E. Cates, Run-and-Tumble Particles with Hydrodynamics: Sedimentation, Trapping, and Upstream Swimming, Phys. Rev. Lett. **104**, 258101 (2010).

[16] J. Tailleur and M. E. Cates, Statistical Mechanics of Interacting Run-and-Tumble Bacteria, Phys. Rev. Lett. **100**, 218103 (2008).

[17] L. Angelani, Run-and-tumble particles, telegrapher's equation and absorption problems with partially reflecting boundaries, J. Phys. A: Math. Theor. **48**, 495003 (2015).

[18] G. Szamel, Self-propelled particle in an external potential: Existence of an effective temperature, Phys. Rev. E **90**, 012111 (2014).

[19] C. Maggi, U. Marini Bettolo Marconi, N. Gnan, and R. di Leonardo, Sci. Rep. **5**, 10742 (2015).

[20] M. R. Shaebani, A. Wysocki, R. G. Winkler, G. Gompper, and H. Rieger, Computational models for active matter, Nat. Rev. Phys. **2**, 181 (2020).

[21] L. Caprini, A. R. Sprenger, H. Löwen, and R. Wittmann, The parental active model: A unifying stochastic description of self-propulsion, J. Chem. Phys. **156**, 071102 (2022).

[22] M. E. Cates and J. Tailleur, Motility-induced phase separation, Annu. Rev. Condens. Matter Phys. **6**, 219 (2015).

[23] B. Liebchen and H. Lowen, Synthetic chemotaxis and collective behavior in active matter, Acc. Chem. Res. **51**, 2982 (2018).

[24] J. Stenhammar, A. Tiribocchi, R. J. Allen, D. Marenduzzo, and M. E. Cates, Continuum Theory of Phase Separation Kinetics for Active Brownian Particles, Phys. Rev. Lett. **111**, 145702 (2013).

[25] P. Hänggi, P. Talkner, and M. Borkovec, Reaction-rate theory: Fifty years after kramers, Rev. Mod. Phys. **62**, 251 (1990).

[26] A. K. Tripathi, T. Das, G. Paneru, H. K. Pak, and T. Tlusty, Acceleration of enzymatic catalysis by active hydrodynamic fluctuations, Commun. Phys. **5**, 101 (2022).

[27] M. M. Salek, F. Carrara, V. Fernandez, J. S. Guasto, and R. Stocker, Bacterial chemotaxis in a microfluidic t-maze reveals strong phenotypic heterogeneity in chemotactic sensitivity, Nat. Commun. **10**, 1877 (2019).

[28] J. Elgeti and G. Gompper, Self-propelled rods near surfaces, Europhys. Lett. **85**, 38002 (2009).

[29] D. Dürr and A. Bach, The Onsager-Machlup function as lagrangian for the most probable path of a diffusion process, Commun. Math. Phys. **60**, 153 (1978).

[30] C. Wissel, Manifolds of equivalent path integral solutions of the fokker-planck equation, Z. Phys. B **35**, 185 (1979).

[31] P. Faccioli, M. Sega, F. Pederiva, and H. Orland, Dominant Pathways in Protein Folding, Phys. Rev. Lett. **97**, 108101 (2006).

[32] A. B. Adib, Stochastic actions for diffusive dynamics: Reweighting, sampling, and minimization, J. Phys. Chem. B **112**, 5910 (2008).

[33] J. Wang, K. Zhang, and E. Wang, Kinetic paths, time scale, and underlying landscapes: A path integral framework to study global natures of nonequilibrium systems and networks, J. Chem. Phys. **133**, 125103 (2010).

[34] L. Onsager and S. Machlup, Fluctuations and irreversible processes, Phys. Rev. **91**, 1505 (1953).

[35] S. Machlup and L. Onsager, Fluctuations and irreversible process. ii. systems with kinetic energy, Phys. Rev. **91**, 1512 (1953).

[36] M. Doi, J. Zhou, Y. Di, and X. Xu, Application of the onsager-machlup integral in solving dynamic equations in nonequilibrium systems, Phys. Rev. E **99**, 063303 (2019).

[37] H. Wang, T. Qian, and X. Xu, Onsager's variational principle in active soft matter, Soft Matter **17**, 3634 (2021).

[38] M. E. Cates, É. Fodor, T. Markovich, C. Nardini, and E. Tjhung, Stochastic hydrodynamics of complex fluids: Discretisation and entropy production, Entropy **24**, 254 (2022).

[39] J. Gladrow, U. F. Keyser, R. Adhikari, and J. Kappler, Experimental Measurement of Relative Path Probabilities and Stochastic Actions, Phys. Rev. X **11**, 031022 (2021).

[40] K. Yasuda, A. Kobayashi, L.-S. Lin, Y. Hosaka, I. Sou, and S. Komura, The onsager–machlup integral for non-reciprocal systems with odd elasticity, J. Phys. Soc. Jpn. **91**, 015001 (2022).

[41] K. Yasuda and K. Ishimoto, The most probable path of an active brownian particle, Phys. Rev. E **106**, 064120 (2022).

[42] L. Dabelow, S. Bo, and R. Eichhorn, Irreversibility in Active Matter Systems: Fluctuation Theorem and Mutual Information, Phys. Rev. X **9**, 021009 (2019).

[43] J. L. Lebowitz and H. Spohn, A gallavotti–cohen-type symmetry in the large deviation functional for stochastic dynamics, J. Stat. Phys. **95**, 333 (1999).

[44] C. Maggi, M. Paoluzzi, N. Pellicciotta, A. Lepore, L. Angelani, and R. Di Leonardo, Generalized Energy Equipartition in Harmonic Oscillators Driven by Active Baths, Phys. Rev. Lett. **113**, 238303 (2014).

[45] C. Maggi, M. Paoluzzi, L. Angelani, and R. Di Leonardo, Memory-less response and violation of the fluctuation-dissipation theorem in colloids suspended in an active bath, Sci. Rep. **7**, 1 (2017).

[46] A. Argun, A.-R. Moradi, E. Pinçe, G. B. Bagci, A. Imparato, and G. Volpe, Non-boltzmann stationary distributions and nonequilibrium relations in active baths, Phys. Rev. E **94**, 062150 (2016).

[47] S. Chaki and R. Chakrabarti, Entropy production and work fluctuation relations for a single particle in active bath, Physica A **511**, 302 (2018).

[48] Y. Fily and M. C. Marchetti, Athermal Phase Separation of Self-Propelled Particles with No Alignment, Phys. Rev. Lett. **108**, 235702 (2012).

[49] M. Paoluzzi, C. Maggi, U. Marini Bettolo Marconi, and N. Gnan, Critical phenomena in active matter, Phys. Rev. E **94**, 052602 (2016).

[50] T. F. F. Farage, P. Krinninger, and J. M. Brader, Effective interactions in active brownian suspensions, Phys. Rev. E **91**, 042310 (2015).

[51] C. Nardini, É. Fodor, E. Tjhung, F. van Wijland, J. Tailleur, and M. E. Cates, Entropy Production in Field Theories without Time-Reversal Symmetry: Quantifying the Non-Equilibrium Character of Active Matter, Phys. Rev. X **7**, 021007 (2017).

[52] U. M. B. Marconi, A. Puglisi, and C. Maggi, Heat, temperature and clausius inequality in a model for active brownian particles, Sci. Rep. **7**, 46496 (2017).

[53] D. Mandal, K. Klymko, and M. R. DeWeese, Mandal, Klymko, and DeWeese Reply, Phys. Rev. Lett. **121**, 139802 (2018).

[54] E. Flenner, G. Szamel, and L. Berthier, The nonequilibrium glassy dynamics of self-propelled particles, Soft Matter **12**, 7136 (2016).

[55] L. Berthier and J. Kurchan, Non-equilibrium glass transitions in driven and active matter, Nat. Phys. **9**, 310 (2013).

[56] S. Shankar and M. C. Marchetti, Hidden entropy production and work fluctuations in an ideal active gas, Phys. Rev. E **98**, 020604(R) (2018).

[57] N. G. Van Kampen, *Stochastic Processes in Physics and Chemistry*, Vol. 1 (Elsevier, New York, 1992).

[58] C. W. Gardiner, *Handbook of Stochastic Methods*, Vol. 3 (Springer, Berlin, 1985).

[59] L. Caprini, F. Cecconi, and U. Marini Bettolo Marconi, Correlated escape of active particles across a potential barrier, J. Chem. Phys. **155**, 234902 (2021).

[60] H. Risken and K. Voigtlaender, Solutions of the fokker-planck equation describing the thermalization of neutrons in a heavy gas moderator, Z. Phys. B **54**, 253 (1984).

[61] L. Dabelow, S. Bo, and R. Eichhorn, How irreversible are steady-state trajectories of a trapped active particle? J. Stat. Mech.: Theory Exp. (2021) 033216.

[62] W. R. Inc., *MATHEMATICA, Version 13.2*, Champaign, IL, 2022.

[63] L. Caprini, Umberto Marini Bettolo Marconi, A. Puglisi, and A. Vulpiani, Comment on Entropy Production and Fluctuation Theorems for Active Matter, Phys. Rev. Lett. **121**, 139801 (2018).

[64] L. Caprini, U. M. B. Marconi, A. Puglisi, and A. Vulpiani, The entropy production of Ornstein–Uhlenbeck active particles: A path integral method for correlations, J. Stat. Mech.: Theory Exp. (2019) 053203.